Functionalized Phosphine–Phosphinimines as Heteroatomic Ligands. Synthesis, Characterization, and Representative X-ray Structures of the Phosphine–Phosphinimines $Ph_2PCH_2PPh_2{=}NAr$ [Ar = 5-F,2,4-$(NO_2)_2C_6H_2$, 4-$(CN)C_6F_4$] and Structure of the Rhodium(I) Complex $Cl(CO)\overline{RhP(Ph)_2CH_2PPh_2{=}NC_6F_4}$-4-CN

Kattesh V. Katti,[1] B. D. Santarsiero,[1] A. Alan Pinkerton,[2] and Ronald G. Cavell*,[1]

Department of Chemistry, University of Alberta, Edmonton, AB, Canada T6G 2G2, and Department of Chemistry, University of Toledo, Toledo, Ohio 43606–3390

Received May 18, 1993®

Reaction of the (trimethylsilyl)phosphinimine–phosphine $Me_3SiN{=}PPh_2CH_2PPh_2$ with nitro-fluoro aromatics and aromatic fluoro nitriles (containing at least one activated fluorine on the position which becomes, as the point of attachment to the imine nitrogen, position 1 of the ring) in refluxing toluene gave the phosphinimine–phosphines $RN{=}PPh_2CH_2PPh_2$ [R = 2,5-$(CN)_2C_6F_3$, 3,4-$(CN)_2C_6F_3$, 5-F-2,4-$(NO_2)_2C_6H_2$, 2,4-$(NO_2)_2C_6H_3$]. The compounds **2** (R = 4-$(CN)C_6F_4$) and **4** (R = 5-F-2,4-$(NO_2)_2C_6H_2$) have been structurally characterized. Data for **2** (at 23 °C): monoclinic, $P2_1/c$ (No. 14), a = 11.065(4) Å, b = 30.218(10) Å, c = 9.302(4) Å, β = 115.37(3)°, V = 2810 Å^3, Z = 4, R_1 = 0.070, R_2 = 0.080. The P=N bond is 1.567(4) Å, and the P^V–N–C(phenyl) angle is 132.9(3)°. The P^{III}–C–P^V angle is 110.9(2)°. Data for **4** (at −80 °C): monoclinic Cc (No. 9), a = 18.957(5) Å, b = 12.783(8) Å, c = 11.607(4) Å, β = 102.87(3)°, V = 2742 Å^3, Z = 4, R_1 = 0.052, R_2 = 0.049. The P=N bond is 1.589(5) Å, and the P^V–N–C(phenyl) angle is 128.8(4)°. The P^V–C–P^{III} angle is 113.2(3)°. In both **2** and **4** the fluoro aromatic ring lies in proximity to one of the phenyl rings on P^{III} and these two rings are eclipsed. These compounds react readily with $[Rh(CO)_2Cl]_2$ to form the chelated Rh complexes of the form $RN{=}\overline{PPh_2CH_2PPh_2Rh(CO)Cl}$ with R as above. The R = 4-$(CN)C_6F_4$ derivative, **10**, has been structurally characterized. Data for **10** (at 21 °C): monoclinic $C2/c$ (No. 15), a = 42.499(4) Å, b = 9.020(1) Å, c = 20.257(2) Å, β = 111.79(1)°, V = 7210.4 Å^3, Z = 8, R_1 = 0.036, R_2 = 0.056. The complex shows the square planar geometry around Rh^I with the CO *cis* to the phosphine. Bond angles and lengths are typical for this square planar chelate complex structure. The P(2)–N(1) distance of 1.616(2) Å in the complex (approximately 0.05 Å longer than that in the free ligand) is normal for a coordinated iminophosphoranyl group. The directly bound Rh–P^{III} distance of 2.2132(8) Å also lies within the range found in many Rh(I) phosphine complexes of the type $P_2Rh(CO)Cl$.

Introduction

Monophosphazenes of the type $R_3P{=}NR'$, commonly referred to as phosphinimines or iminophosphoranes, show a variety of bonding modes with the early and late transition metals and with actinides.[3-10] These versatile ligands, which may also function as uninegative anions (i.e., $R_3P{=}N^-$), can donate 1, 2, or 4 electrons to the metal center. Under the right circumstances, therefore, there can be considerable multiple bond character in the M–N bond in $R_3P{=}N{-}M$ complexes.[7-11] Subtle changes in the basicities of the iminato nitrogen can be effected by the appropriate choice of the substituents on the phosphorus (R) or the nitrogen (R′). The introduction of a second phosphine moiety on the phosphinimine backbone presents the further possibility of developing a new class of heterodifunctional phosphine–phosphinimine ligand systems of the type A wherein the backbones can encompass a variety of bridging species (Q), such as CH_2, $(CH_2)_n$, *o*-C_6H_4, etc., spanning a range of connecting components including assemblies of saturated or unsaturated character.

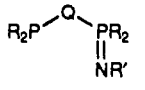

A

We have recently shown that the controlled oxidation of the readily available bis(diphenylphosphino)methane (dppm) with azidotrimethylsilane produces the heterodifunctional phosphine–phosphinimine **1** in good yields (eq 1).[11-15] This route, applicable

$$Ph_2PCH_2PPh_2 + Me_3SiN_3 \xrightarrow[-N_2]{} Ph_2PCH_2PPh_2{=}NSiMe_3 \quad (1)$$
$$\mathbf{1}$$

to a variety of bridged diphosphorus compounds, provides ready access to substituted phosphoranimine–phosphines. Ligands of the type **1** are versatile because they combine the ligating properties of the phosphinimines and those of the traditional tertiary phosphines. In recent studies, we have demonstrated the efficacy of using the heterodifunctional ligands of this type for the following: (i) the production of metal chelates with the early and

• Abstract published in *Advance ACS Abstracts*, October 15, 1993.

(1) University of Alberta.
(2) University of Toledo.
(3) Abel, E. W.; Mucklejohn, S. A. *Phosphorus Sulfur* **1981**, *9*, 235.
(4) Dehnicke, K.; Strähle, J. *Polyhedron* **1989**, *8*, 707.
(5) Dehnicke, K.; Strähle, J. *Angew. Chem., Int. Ed. Engl.* **1992**, *31*, 955.
(6) Bakir, M.; White, P. S.; Dovletoglou, A.; Meyer, T. J. *Inorg. Chem.* **1991**, *30*, 2835.
(7) Roesky, H. W.; Katti, K. V.; Seske, U., Herbst, R.; Egert, E.; Sheldrick, G. M. *Z. Naturforsch.* **1986**, *41B*, 1509.
(8) Fenske, D.; Böhm, E.; Dehnicke, K.; Strähle, J. *Z. Naturforsch.* **1988**, *43B*, 1.
(9) Cramer, R. E.; Edelmann, F.; Mori, A. L.; Roth, S.; Gilje, J. W.; Tatsumi, K.; Nakamura, A. *Organometallics* **1988**, *7*, 841.
(10) Roesky, H. W.; Seseke, U.; Noltemeyer, M.; Jones, P. G.; Sheldrick, G. M. *J. Chem. Soc., Dalton Trans.* **1986**, 1309.
(11) Katti, K. V.; Cavell, R. G. *Inorg. Chem.* **1989**, *28*, 3033.
(12) Katti, K. V.; Cavell, R. G. *Organometallics* **1989**, *8*, 2147.
(13) Katti, K. V.; Cavell, R. G. *Organometallics* **1988**, *7*, 2236.
(14) Katti, K. V.; Batchelor, R. J.; Einstein, F. W. B.; Cavell, R. G. *Inorg. Chem.* **1990**, *29*, 808.
(15) Katti, K. V.; Cavell, R. G. *Comments Inorg. Chem.* **1990**, *10*, 53.

0020-1669/93/1332-5919$04.00/0

Table I. Phosphorus-31 NMR[a] Data for Phosphine–Phosphinimines **1–6** and Their Metal Complexes (**7–11**)

compd[b]	no.	$\delta(P^{III})$	$\delta(P^{V})$	$^2J_{PP}$, Hz	J_{PRh}, Hz	ref
$Me_3SiN{=}PPh_2CH_2PPh_2$	**1**	−28.20	−1.40	57.7		12
$4\text{-}CNC_6F_4N{=}PPh_2CH_2PPh_2$	**2**	−30.12	13.04	53.6		16
$2,4\text{-}(NO_2)_2C_6H_3N{=}PPh_2CH_2PPh_2$	**3**	−29.59	10.12	53.5		
$5\text{-}F,2,4\text{-}(NO_2)_2C_6H_2N{=}PPh_2CH_2PPh_2$	**4**	−30.12	11.50	53.9		
$2,5\text{-}(CN)_2C_6F_3N{=}PPh_2CH_2PPh_2$[c]	**5**	−30.34	11.50	53.0		
$3,4\text{-}(CN)_2C_6F_3N{=}PPh_2CH_2PPh_2$[d]	**6**	−30.7	14.20	53.2		
$(NO_2)_2C_6H_3N{=}PPh_2CH_2PPh_2Rh(CO)Cl$	**7**	39.60	41.85	30.1	$^1J_{PRh}$ = 166.8[e]	
$(NO_2)_2C_6FH_2N{=}PPh_2CH_2PPh_2Rh(CO)Cl$	**8**	39.72	42.70	30.2	$^1J_{PRh}$ = 164.0 $^2J_{PRh}$ = 7.0	
$(CN)_2C_6F_3N{=}PPh_2CH_2PPh_2Rh(CO)Cl$	**9**	40.05	43.70	30.1	$^1J_{PRh}$ = 166.8 $^2J_{PRh}$ = 6.2	
$CNC_6F_4N{=}PPh_2CH_2PPh_2Rh(CO)Cl$	**10**	39.75	43.70	30.8	$^1J_{PRh}$ = 165.2[e]	12
$Me_3SiN{=}PPh_2CH_2PPh_2Rh(CO)Cl$	**11**	37.64	24.36	31.1	$^1J_{PRh}$ = 168.6 $^2J_{PRh}$ = 4.0	12

[a] Spectra obtained in $CDCl_3$ solution; ppm vs 85% H_3PO_4. [b] The substituted aromatics are numbered starting from one at the imine attachment point. The numbers associated with the substituents may therefore be different from those used for the systematic name of the original fluoro aromatic. [c] $^6J_{P^{III}F}$ = 3.9 Hz; $^4J_{P^VF}$ = 10.45 Hz; $^6J_{P^VF}$ = 4.5 Hz. [d] $^4J_{P^VF_o} \sim {}^4J_{P^VF_o}$ = 5.4 Hz; each component appears as a triplet. [e] $^2J_{PRh}$ not observed.

Scheme I

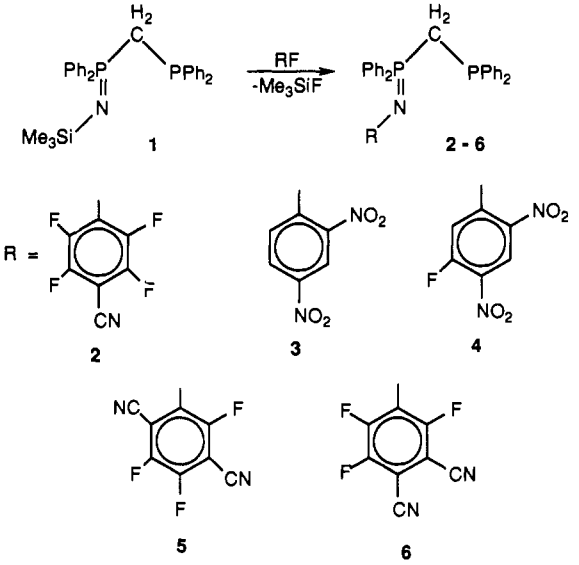

late transition metals;[11-15] (ii) the formation of complexes with M–N σ bonds;[12-16] (iii) the development of mixed early and late transition metal heterobimetallic compounds.[17]

Herein, we extend a simple synthetic strategy[12] to produce substituted heterodifunctional ligands of the type A which possess different basicity at the phosphinimine nitrogen center obtained through an easy substitution reaction at the silylated imine nitrogen. The structure characteristics of two members of this class of ligand are reported as is their reactivity with Rh(I) precursors to produce metal chelates of the general formula $ArN{=}PPh_2CH_2PPh_2Rh(CO)Cl$. A structurally characterized example of one Rh(I) complex is described.

Results and Discussion

Synthesis, Properties, and Structure of N-Substituted Phosphinimine–Phosphines. The reaction of the trimethylsilyl phosphinimine phosphine $Me_3SiN{=}PPh_2CH_2PPh_2$, **1**, with fluoro aromatics containing nitrile and nitro substituents in refluxing toluene gave the phosphinimine–phosphines **2–6** in good yields (Scheme I). These heteroatomic multifunctional compounds **2–6** are crystalline, air-stable solids which are highly soluble in most common organic solvents. The reactions shown in Scheme I demonstrate the facile displacement of single aromatic C–F bonds, and all the reactions are regiospecific. In all cases investigated herein only one fluorine was replaced. The most reactive situation is that in which the displaced fluorine is located *para* to an electron-withdrawing activating group, and most of the examples considered herein represent this situation. Thus the fluorine *para* to CN in $C_6F_5(CN)$ was eliminated to bind the fluoro aromatic to the imine.[12] Second substitution was not observed. Reactions of fluoro aromatics which contained two activating groups positioned so that, in principle, two fluorine atoms could be replaced, for example $1,5\text{-}(F)_2\text{-}2,4\text{-}(NO_2)_2C_6H_2$ and $1,2\text{-}(CN)_2C_6F_4$, gave **4** and **6**, respectively, in which only one fluorine was replaced. This specificity, first demonstrated in the case of C_5F_5N and the synthesis of **2** reported earlier, appears to be reasonably general in this system although there is apparently no reason why further substitution cannot be effected.[12] A fluorine *ortho* to the activating group can be replaced when no *para* fluorine is present as in $1,4\text{-}(CN)_2C_6F_4$, which gave only **5** and no evidence of disubstitution. The aromatic compound need contain only one activated fluorine as demonstrated by the reaction of $1\text{-}F\text{-}2,4\text{-}(NO_2)_2C_6H_3$; in this case the product, **3**, carries no fluorine substituents on the aromatic ring. This reaction also provides a safe route to nitro aromatic iminophosphorano phosphines such as **3** and **4**, which are, in principle, also accessible through monooxidation of the appropriate bis(phosphines) with the appropriate azide (the Staudinger reaction). Attaching a nitro aromatic to the desired phosphorus imide center through the reaction of the nitro fluoro aromatic with the iminosilylated bis(phosphorus) compound *via* the elimination of Me_3SiF however avoids the need for preparation of the nitro aromatic azide, which would be required for the Staudinger route.

The identification and molecular constitution of **3–6** follows from the analytical data, mass spectra, and ^1H, ^{31}P, and ^{19}F NMR spectroscopy. Molecular ions for each of the compounds **3–6** were observed in the mass spectra as was the case for **2**.[12] Phosphorus-31 NMR data are given in Table I. The ^{31}P spectra of all of these compounds consist of two sharp doublets which are readily assigned to the phosphine (PPh_2) and the phosphoranimine ($N{=}PPh_2$–) groups, respectively. The P^{III} center lies typically to high field of the P^V center, and the shift difference is of the order of 20 ppm. The introduction of an electron-withdrawing nitro or cyano fluoro aromatic at the phosphinimine nitrogen, as in **2–6**, causes a significant deshielding of the oxidized phosphorus and also produces a modest decrease ($\sim$3 Hz) in the $^2J_{PP}$ values in all these compounds compared to **1** (Table I).

Phosphinimines of the type $R_3P{=}NSiMe_3$ are readily hydrolyzed, and the resulting reactions ultimately produce phosphine oxide (i.e. $R_3P{=}O$) as the sole product. Substitution of the $SiMe_3$

(16) Katti, K. V.; Cavell, R. G. *Inorg. Chem.* **1989**, *28*, 413.
(17) Katti, K. V.; Cavell, R. G. *Organometallics* **1991**, *10*, 539.

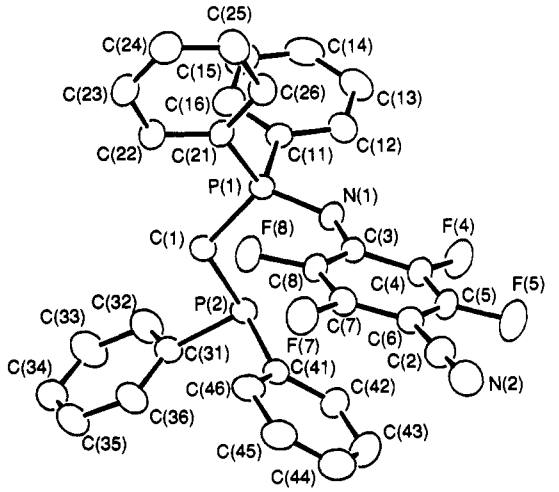

Figure 1. Perspective view of **2**, showing the atom-numbering scheme. Atoms are represented by Gaussian ellipsoids[19] at the 20% probability level. Hydrogen atoms are omitted for clarity.

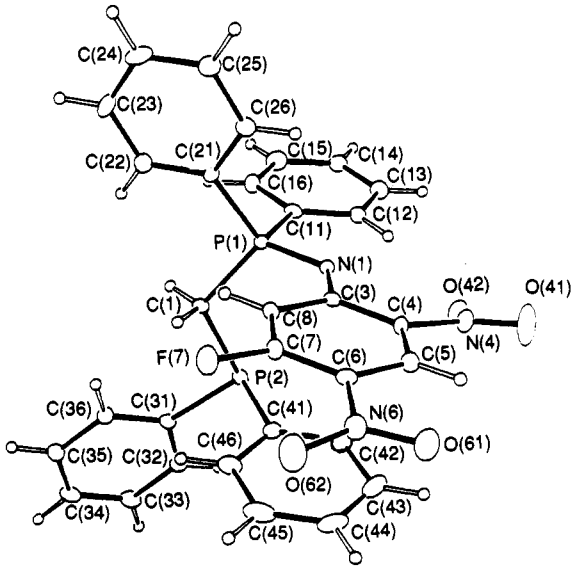

Figure 2. Perspective view of **4**, showing the atom-labeling scheme. Atoms are represented by Gaussian ellipsoids[19] at the 20% probability level except for hydrogen atoms which are shown artificially small. Some hydrogen atoms have been omitted for clarity.

group by an aromatic functionality as in **2**–**6** reduces the rate of hydrolysis significantly. Additional potentially useful features for these compounds are the nitrile and nitro functions on the aromatic substituents, which may open further avenues for complexation chemistry. It is worth noting that few substituted nitro aromatics have been available for complexation to transition metals.

X-ray structures have been determined for **2**[12,18] and **4**[18] as representative examples of these new phosphine–phosphinimines. The ORTEP[19] plots for **2** and **4** are shown in Figures 1 and 2, respectively. The selected bonding parameters and the X-ray crystallographic data appear in Tables II–V. The P–N bond lengths (1.576(4) Å for **2** and 1.589(5) Å for **4**) fall within the range observed for phosphinimines and phosphazene compounds with P–N double bonds. The P–N bond lengths in **2** or **4** are also substantially longer than the P=N bond length in $Me_3SiN{=}PPh_2CH_2PPh_2$ (**1**) (1.529(3) Å)[20] and follow the general trend of shorter P=N bonds and wider P–N–X angles for iminophosphoranes carrying the silyl substituent compared to those with

(18) Structure done at the University of Alberta.
(19) Johnson, C. K. ORTEP, Report ORNL No. 5138, Oak Ridge National Laboratory, Oak Ridge, TN, 1976.
(20) Schmidbaur, H.; Bowmaker, G. A.; Kumberger, O.; Müller, G.; Wolfsberger, W. *Z. Naturforsch., B* **1990**, *45b*, 476.

Table II. Summary of Crystallographic Data

	2	**4**	**10**·$CHCl_3$
formula	$C_{32}H_{22}F_4N_2P_2$	$C_{31}H_{24}FN_3O_4P_2$	$C_{33}H_{22}ClRhF_4N_2OP_2{\cdot}CHCl_3$
fw	572.49	583.50	858.23
space group	monoclinic, $P2_1/c$ (No. 14)	monoclinic, Cc (No. 9)	monoclinic, $C2/c$ (No. 15)
a, Å	11.065(4)	18.957(5)	42.499(4)
b, Å	30.218(10)	12.783(8)	9.020(1)
c, Å	9.302(4)	11.607(4)	20.257(2)
β, deg	115.37(3)	102.87(3)	111.79(1)
V, Å^3	2810	2742	7210.4
Z	4	4	8
λ, Å	0.710 73 (Mo K$\bar{\alpha}$)	0.710 73 (Mo K$\bar{\alpha}$)	0.709 30 (Mo Kα_1)
temp, °C	23	−80	21
d_{calcd}, g/cm^3	1.352	1.413	1.58
cryst size, mm	0.3 × 0.3 × 0.5	0.1 × 0.1 × 0.4	0.36 × 0.35 × 0.10
μ, cm^{-1}	1.99	2.11	9.0
no. of variables	361	368	433
R_1[a]	0.070	0.052	0.036
R_2[b]	0.080	0.049	0.056

[a] $R_1 = \sum||F_o| - |F_c||/\sum|F_o|$. [b] $R_2 = [\sum w(|F_o| - |F_c|)^2/\sum wF_o^2]^{1/2}$.

Table III. Atomic Coordinates and Equivalent Isotropic Displacement Parameters[a,b] (Å^2) for **2**

atom	x	y	z	B_{eq}
P(1)	0.1583(1)	0.07755(4)	0.9338(1)	4.60(3)
P(2)	0.0966(1)	0.14031(5)	0.6589(2)	5.21(4)
F(4)	−0.2609(3)	0.0627(1)	0.7450(4)	8.6(1)
F(5)	−0.4285(3)	0.0986(1)	0.8519(5)	9.6(1)
F(7)	−0.0730(3)	0.1759(1)	1.2414(4)	8.0(1)
F(8)	0.0960(2)	0.1410(1)	1.1397(3)	6.80(9)
N(1)	0.0044(3)	0.0765(1)	0.8870(4)	5.0(1)
N(2)	−0.4202(4)	0.1698(2)	1.1479(6)	9.1(2)
C(1)	0.2144(4)	0.1259(2)	0.8670(5)	5.2(1)
C(2)	−0.3458(5)	0.1559(2)	1.1052(6)	6.9(2)
C(3)	−0.0739(4)	0.0981(2)	0.9430(5)	4.7(1)
C(4)	−0.2125(5)	0.0907(2)	0.8721(6)	5.7(2)
C(5)	−0.2969(4)	0.1096(2)	0.9247(6)	5.9(2)
C(6)	−0.2558(4)	0.1383(2)	1.0499(6)	5.6(2)
C(7)	−0.1213(5)	0.1475(2)	1.1182(6)	5.5(2)
C(8)	−0.0339(4)	0.1285(2)	1.0690(6)	5.0(1)
C(11)	0.1892(4)	0.0311(2)	0.8330(5)	4.6(1)
C(12)	0.0865(5)	0.0032(2)	0.7417(6)	6.2(2)
C(13)	0.1124(6)	−0.0341(2)	0.6698(6)	7.3(2)
C(14)	0.2410(6)	−0.0420(2)	0.6902(6)	7.7(2)
C(15)	0.3429(6)	−0.0145(2)	0.7798(6)	7.4(2)
C(16)	0.3173(5)	0.0224(2)	0.8520(6)	6.4(2)
C(21)	0.2662(4)	0.0696(2)	1.1421(5)	4.6(1)
C(22)	0.3850(4)	0.0930(2)	1.2230(6)	5.5(2)
C(23)	0.4599(5)	0.0849(2)	1.3849(6)	6.1(2)
C(24)	0.4172(5)	0.0554(2)	1.4631(6)	6.8(2)
C(25)	0.3022(6)	0.0326(2)	1.3834(6)	7.8(2)
C(26)	0.2248(5)	0.0392(2)	1.2228(6)	6.7(2)
C(31)	0.2026(4)	0.1809(2)	0.6225(5)	5.4(2)
C(32)	0.2762(5)	0.1652(2)	0.5457(7)	8.9(2)
C(33)	0.3651(6)	0.1921(2)	0.5165(9)	11.3(3)
C(34)	0.3827(6)	0.2347(2)	0.5652(8)	8.9(2)
C(35)	0.3101(6)	0.2507(2)	0.6358(7)	8.0(2)
C(36)	0.2179(6)	0.2244(2)	0.6655(7)	7.3(2)
C(41)	−0.0282(4)	0.1741(2)	0.6877(5)	5.2(1)
C(42)	−0.1579(5)	0.1710(2)	0.5680(7)	6.9(2)
C(43)	−0.2608(6)	0.1949(2)	0.5801(8)	9.5(3)
C(44)	−0.2342(6)	0.2208(2)	0.7093(9)	9.8(3)
C(45)	−0.1089(5)	0.2244(2)	0.8263(8)	8.0(2)
C(46)	−0.0049(5)	0.2011(2)	0.8183(6)	6.5(2)

[a] Numbers in parentheses are estimated standard deviations in the least significant digits. [b] All non-hydrogen atoms were refined anisotropically. Displacement parameters for the anisotropically refined atoms are given in the form of the equivalent isotropic Gaussian displacement parameter, B_{eq}, defined as $^4/_3[a^2\beta_{11} + b^2\beta_{22} + c^2\beta_{33} + ac(\cos\beta)\beta_{13}]$.

Table IV. Atomic Coordinates and Equivalent Isotropic Displacement Parameters[a,b] (Å²) for **4**

atom	x	y	z	B_{eq}
P(1)	0.2500	0.3254(1)	0.2500	1.64(3)
P(2)	0.37188(9)	0.4558(1)	0.4009(2)	2.03(3)
F(7)	0.4196(2)	-0.0033(3)	0.3026(3)	3.5(1)
O(41)	0.2122(3)	0.0753(4)	0.6353(4)	5.5(1)
O(42)	0.2138(3)	0.2314(3)	0.5703(4)	3.4(1)
O(61)	0.3941(3)	-0.1642(4)	0.5950(4)	3.8(1)
O(62)	0.4604(3)	-0.1369(4)	0.4695(5)	5.1(1)
N(1)	0.2463(2)	0.2497(4)	0.3571(4)	1.6(1)
N(4)	0.2320(3)	0.1397(4)	0.5706(4)	2.7(1)
N(6)	0.4096(3)	-0.1145(4)	0.5132(4)	2.7(1)
C(1)	0.3359(3)	0.3895(5)	0.2571(5)	1.9(1)
C(3)	0.2845(3)	0.1619(5)	0.3919(5)	1.7(1)
C(4)	0.2777(3)	0.1042(5)	0.4937(5)	1.8(1)
C(5)	0.3160(3)	0.0137(5)	0.5289(5)	2.2(1)
C(6)	0.3654(3)	-0.0235(5)	0.4680(5)	2.1(1)
C(7)	0.3733(3)	0.0308(5)	0.3668(5)	2.3(1)
C(8)	0.3338(3)	0.1178(5)	0.3296(5)	1.9(1)
C(11)	0.1851(3)	0.4269(5)	0.2568(5)	2.0(1)
C(12)	0.1487(3)	0.4265(5)	0.3459(5)	2.2(1)
C(13)	0.0955(3)	0.5018(5)	0.3474(6)	3.1(2)
C(14)	0.0801(3)	0.5779(5)	0.2596(6)	2.8(2)
C(15)	0.1184(4)	0.5787(6)	0.1710(6)	3.5(2)
C(16)	0.1706(3)	0.5034(5)	0.1683(6)	2.7(2)
C(21)	0.2262(3)	0.2680(5)	0.1051(5)	1.8(1)
C(22)	0.2502(3)	0.3043(5)	0.0085(5)	2.8(2)
C(23)	0.2272(4)	0.2576(6)	-0.1017(6)	3.6(2)
C(24)	0.1804(4)	0.1734(6)	-0.1147(6)	3.7(2)
C(25)	0.1568(4)	0.1359(6)	-0.0190(6)	3.2(2)
C(26)	0.1793(3)	0.1824(5)	0.0903(6)	2.7(2)
C(31)	0.4523(3)	0.5187(4)	0.3685(5)	1.9(1)
C(32)	0.4822(3)	0.5988(5)	0.4459(6)	2.6(2)
C(33)	0.5447(3)	0.6498(5)	0.4326(6)	2.9(2)
C(34)	0.5771(3)	0.6226(5)	0.3423(6)	3.0(2)
C(35)	0.5472(3)	0.5448(5)	0.2639(6)	2.8(2)
C(36)	0.4857(3)	0.4929(5)	0.2783(5)	2.4(2)
C(41)	0.4125(3)	0.3461(5)	0.4947(5)	2.3(2)
C(42)	0.3844(4)	0.3230(5)	0.5927(6)	3.4(2)
C(43)	0.4135(4)	0.2443(6)	0.6700(7)	4.5(2)
C(44)	0.4718(4)	0.1863(6)	0.6484(7)	4.7(2)
C(45)	0.5008(4)	0.2093(6)	0.5532(8)	4.3(2)
C(46)	0.4710(4)	0.2901(5)	0.4756(7)	3.2(2)

[a] Numbers in parentheses are estimated standard deviations in the least significant digits. [b] All non-hydrogen atoms were refined anisotropically. Displacement parameters for the anisotropically refined atoms are given in the form of the equivalent isotropic Gaussian displacement parameter, B_{eq}, defined as $^4/_3[a^2\beta_{11} + b^2\beta_{22} + c^2\beta_{33} + ac(\cos\beta)\beta_{13}]$.

Table V. Selected Bond Distances[a] (Å), Angles[a] (deg), and Inter-Ring Spacings[a] (Å) for Compounds **2** and **4**

2		**4**	
	Distances		
P(1)-C(1)	1.800(5)	P(1)-C(1)	1.808(6)
P(1)-N(1)	1.567(4)	P(1)-N(1)	1.589(5)
P(2)-C(1)	1.863(4)	P(2)-C(1)	1.860(6)
N(1)-C(3)	1.354(7)	N(1)-C(3)	1.348(7)
	Angles		
C(1)-P(1)-N(1)	114.5(2)	C(1)-P(1)-N(1)	115.9(3)
P(1)-N(1)-C(3)	132.9(3)	P(1)-N(1)-C(3)	128.8(4)
P(1)-C(1)-P(2)	110.9(2)	P(1)-C(1)-P(2)	113.2(3)
	Important Interatomic Spacings of Eclipsed Rings[b]		
C(3)-C(41)	3.494(8)	C(3)-C(41)	3.401(8)
C(4)-C(42)	3.966(9)	C(4)-C(42)	3.493(8)
C(5)-C(43)	4.26(1)	C(5)-C(43)	3.666(5)
C(6)-C(44)	4.12(1)	C(6)-C(44)	3.710(5)
C(7)-C(45)	3.622(9)	C(7)-C(45)	3.660(5)
C(8)-C(46)	3.317(8)	C(8)-C(46)	3.539(6)

[a] Numbers in parentheses are estimated standard deviations in the least significant digits. [b] In **2**, the rings deviate from a parallel relationship by 19°; in **4**, the rings deviate from a parallel relationship by 8°.

organo substituents,[21] even those organo substituents such as the strongly electron-withdrawing fluoro aromatics prepared herein.

Scheme II

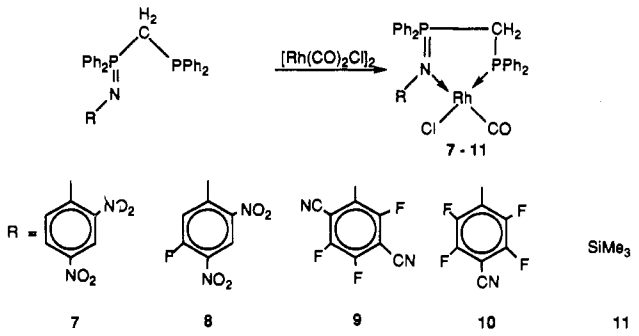

A curious and notable feature of both of these molecules is the proximity of the imine substituent to one of the phenyl rings on the P^{III} and the eclipsed and proximate relationship of these two rings. Diagnostic interatomic spacings are given in Table V. In the case of **4** the aligned rings are roughly parallel, deviating from the parallel relationship by only 8°. The C(phenyl) to C(nitro aromatic) distances range from 3.36 to 3.91 Å. The relative orientation is such that the C atoms on one ring lie between those of the other so each ring carbon has two nearest neighbors within the distance range given. Although two NO_2 and one F would exert a strong electron-withdrawing effect on the ring, it is not clear whether this makes the imine ring sufficiently acidic to act as an acceptor toward the phenyl on P^{III}.

Complexation Reactions of 2–5 with $[Rh(CO)_2Cl]_2$. Formation of Cyclometallaphosphinimine Phosphines of Rh(I). Reactions of **2–5** with $[Rh(CO)_2Cl]_2$ in CH_2Cl_2 at 25 °C gave the complexes $RN{=}PPh_2CH_2PPh_2Rh(CO)Cl$ (R = $C_6H_3(NO_2)_2$ (**7**), $C_6H_2F(NO_2)_2$ (**8**), $C_6F_3(CN)_2$ (**9**), C_6F_4CN (**10**)[12]) in nearly quantitative yields (Scheme II). These complexes can be compared to the complex of the (silylimino)phosphorano phosphine, **11**, described earlier.[12] All of the complexes carrying an aromatic substituent on the imine show marked low-field coordination shifts, of the order of 60 ppm for the P^{III} and approximately 30 ppm for the P^V centers. Furthermore the chemical shift difference between P^{III} and P^V is markedly reduced from ca. 40 ppm to 2–3 ppm. In contrast, the coordination shifts developed by complexes of the trimethylsilyl ligand **1** are comparable at P^{III} (which is to be expected since P^{III} is directly bound to Rh) but only ca. 25 ppm at P^V. As a result, therefore, complex **11** shows substantially different P^{III} and P^V environments. These small differences in the chemical shifts of formally different valence states of P(III) and P(V) centers in the complexes of the fluoro and nitro aromatic ligands **7–10** appear to be unprecedented and suggest that significant single bond character has developed in the P^V–N bond (as witnessed by the length of 1.61 Å for this bond) and perhaps some phosphonium ion character for P^V. Fortunately, the proximity of the phosphorus shifts was not sufficient to introduce second-order character into the ^{31}P NMR spectra; all were first order and easily analyzed. The electronically demanding fluoro aromatic or nitro aromatic substituents contained in **2–6** therefore have a notable effect on the chemistry of the imine nitrogen, in all probability reducing the basicity of the iminato nitrogen which in turn results in a substantial decrease in the strength of the donation of electron density from the iminato nitrogen to the Rh(I) center in the complexes **7–10**. Additional electron density from the electron-rich Rh(I) center may be transmitted through the iminato nitrogen and further delocalized within the fluoro aromatic or the nitro aromatic substituent in complexes **7–10**. These electronic effects may operate in a synergic fashion within the chelate rings of complexes **7–10** and may result in poorer back-bonding of Rh(I) with the P(III) phosphine group in these complexes. Such effects may be the

(21) Reed, R. W.; Cavell, R. G. Unpublished data.

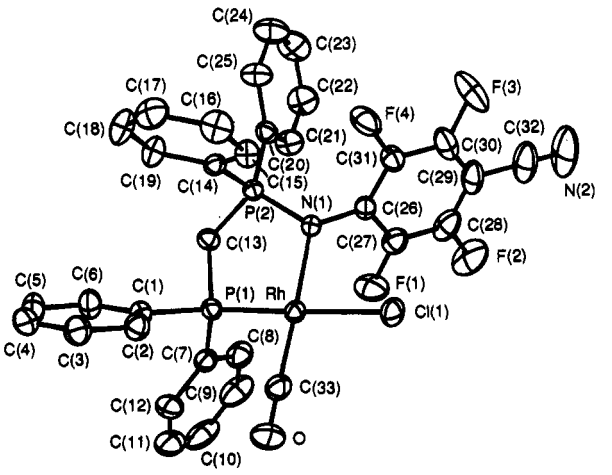

Figure 3. Perspective view of **10**, showing the atom-numbering scheme. Atoms are represented by Gaussian ellipsoids[19] at the 50% probability level. Hydrogen atoms are omitted for clarity.

source of the unusual proximity of the chemical shifts for the two kinds of phosphorus centers noted in complexes **7–10**. Similar electronic effects arising from the fluoro aromatic substituents may be responsible for the notable hydrolytic stability of **2–6**, and this delocalization effect may also be responsible for the observation that the P^V centers in these fluoro aromatic complexes are significantly less shielded (with ^{31}P chemical shifts appearing in the range of 10–15 ppm) relative to the (trimethylsilyl)imine **1** (which appears at −1.4 ppm in the phosphorus NMR spectrum).

Further characterization of the Rh(I) metallacyclic compounds was provided by ^{13}C NMR spectroscopy which showed $^2J_{CP}$ values of 18.75, 19.20, 19.20, and 20.15 Hz, respectively, for **7–10**, indicative of a *cis* relationship between the CO and the phosphine (PPh_2) groups in all the metallacyclic complexes. In addition, CO stretching frequencies of 1970, 1975, 1970, and 1978 cm^{-1} for **7–10**, respectively, are consistent with the proposed *cis* structures.

As a representative example, the X-ray crystal structure of **10**[22] was obtained. An ORTEP[19] plot is shown in Figure 3. The structural parameters are given in Table VI, and the bonding parameters are listed in Table VII. The structure comprises the neutral monomeric complex *p*-$CNC_6F_4\overline{N{=}PPh_2CH_2PPh_2}Rh$-(CO)Cl, **10**, with a cocrystallized molecule of chloroform. The structure shows Rh in a typical square planar environment with the ligand bonded to Rh via N(1) and P(1) to form a five-membered ring. The P(2)–N(1) distance of 1.616(2) Å, which is a normal value for a coordinated iminophosphoranyl group, is approximately 0.05 Å longer than that in the free ligand **2** (Tables III–V). The Rh–P(1) distance of 2.2132(8) Å lies toward the short end of the range found for a number of Rh(I) phosphine complexes (2.23–2.35),[23-29] but this is not unexpected in view of the fact that there are two electronegative atoms as well as CO bound to Rh. The CO is cis to the phosphine as deduced from NMR and IR.

Conclusions

A variety of aromatic substituted phosphorano phosphinimines can be obtained by simple substitution of the $SiMe_3$ group on the parent compound using an activated fluoro aromatic (i.e. a fluoro aromatic with electron-withdrawing substituents on the ring) via elimination of Me_3SiF. The principal reaction site is the site *para* to the activating group; however, other sites may be activated.

Table VI. Atomic Coordinates and Equivalent Isotropic Displacement Parameters[a,b] (Å²) for **10**

atom	*x*	*y*	*z*	B_{eq}
Rh	0.152531(5)	0.02163(2)	0.12099(1)	2.866(4)
Cl(1)	0.13708(2)	0.25702(8)	0.15395(4)	4.36(2)
Cl(2)[c]	0.86191(4)	0.3920(2)	0.54551(7)	9.51(4)
Cl(3)[c]	0.92733(4)	0.4216(2)	0.54205(9)	11.18(5)
Cl(4)[c]	0.91129(5)	0.1657(2)	0.60438(6)	15.72(6)
P(1)	0.16412(2)	−0.19938(8)	0.08828(3)	2.95(1)
P(2)	0.12251(2)	−0.25442(8)	0.17267(3)	2.82(1)
F(1)	0.07300(6)	0.0258(3)	0.0191(1)	7.01(7)
F(2)	0.01417(6)	0.1614(3)	−0.0021(1)	9.61(8)
F(3)	0.03051(5)	0.0875(4)	0.2378(1)	9.49(7)
F(4)	0.08930(5)	−0.0477(3)	0.25900(9)	6.25(6)
O	0.20560(6)	0.1552(3)	0.0788(1)	6.79(7)
N(1)	0.11416(5)	−0.0831(3)	0.1494(1)	3.11(5)
N(2)	−0.03684(9)	0.2499(5)	0.0910(3)	12.5(2)
C(1)	0.20557(6)	−0.2815(3)	0.1338(1)	3.49(6)
C(2)	0.23125(7)	−0.1976(4)	0.1817(1)	4.11(7)
C(3)	0.26329(8)	−0.2610(4)	0.2166(2)	4.74(8)
C(4)	0.26964(8)	−0.4036(4)	0.2029(2)	5.01(8)
C(5)	0.24437(8)	−0.4867(4)	0.1552(2)	5.39(9)
C(6)	0.21212(8)	−0.4269(4)	0.1207(2)	4.54(7)
C(7)	0.15659(7)	−0.2191(3)	−0.0057(1)	3.77(6)
C(8)	0.12364(9)	−0.2137(4)	−0.0555(2)	5.22(9)
C(9)	0.1172(1)	−0.2244(5)	−0.1270(2)	7.2(1)
C(10)	0.1445(1)	−0.2353(5)	−0.1499(2)	8.3(1)
C(11)	0.1768(1)	−0.2351(5)	−0.1011(2)	7.6(1)
C(12)	0.18362(9)	−0.2290(4)	−0.0285(2)	5.61(8)
C(13)	0.13501(6)	−0.3343(3)	0.1048(1)	3.28(6)
C(14)	0.15690(6)	−0.2737(3)	0.2567(1)	3.10(6)
C(15)	0.16373(7)	−0.1599(4)	0.3059(1)	3.81(7)
C(16)	0.18882(8)	−0.1778(4)	0.3732(2)	4.98(8)
C(17)	0.20769(8)	−0.3055(4)	0.3899(2)	5.17(9)
C(18)	0.20117(9)	−0.4165(4)	0.3407(2)	5.53(9)
C(19)	0.17568(8)	−0.4040(4)	0.2740(2)	4.57(8)
C(20)	0.08643(6)	−0.3508(3)	0.1760(1)	3.28(6)
C(21)	0.05704(8)	−0.3606(4)	0.1152(2)	4.81(8)
C(22)	0.02821(9)	−0.4245(5)	0.1178(2)	6.1(1)
C(23)	0.02869(9)	−0.4815(5)	0.1806(2)	7.0(1)
C(24)	0.0571(1)	−0.4754(5)	0.2411(2)	6.6(1)
C(25)	0.08634(7)	−0.4109(4)	0.2391(2)	4.87(8)
C(26)	0.08347(7)	−0.0148(3)	0.1406(1)	3.35(6)
C(27)	0.06307(8)	0.0421(4)	0.0742(2)	4.66(8)
C(28)	0.03277(8)	0.1124(5)	0.0642(2)	6.2(1)
C(29)	0.02095(8)	0.1273(4)	0.1172(2)	5.9(1)
C(30)	0.04078(8)	0.0735(5)	0.1825(2)	5.73(9)
C(31)	0.07098(8)	0.0037(4)	0.1936(2)	4.31(7)
C(32)	−0.0117(1)	0.1958(5)	0.1030(3)	8.4(1)
C(33)	0.18528(7)	0.1039(4)	0.0959(2)	4.22(7)
C(34)[c]	0.8965(1)	0.2950(5)	0.5388(2)	6.9(1)

[a] Standard deviations are given in parentheses. [b] All non-hydrogen atoms were refined anisotropically. Displacement parameters for the anisotropically refined atoms are given in the form of the equivalent isotropic Gaussian displacement parameter, B_{eq}, defined as $^4/_3[a^2\beta_{11} + b^2\beta_{22} + c^2\beta_{33} + ac(\cos\beta)\beta_{13}]$. [c] Chloroform.

Table VII. Selected Bond Distances[a] (Å) and Angles[a] (deg) in the Complex **10**

		Distances	
Rh–Cl(1)	2.3896(8)	P(1)–C(13)	1.853(3)
Rh–P(1)	2.2132(8)	P(2)–C(13)	1.798(3)
Rh–N(1)	2.141(2)	Rh–C(33)	1.809(4)
P(2)–N(1)	1.616(2)	O–C(33)	1.141(5)
		Angles	
Cl(1)–Rh–P(1)	177.13(3)	N(1)–Rh–C(33)	178.0(1)
Cl(1)–Rh–N(1)	90.07(7)	Rh–P(1)–C(13)	107.4(1)
Cl(1)–Rh–C(33)	91.9(1)	Rh–N(1)–P(2)	113.2(1)
P(1)–Rh–N(1)	87.68(7)	Rh–C(33)–O	178.7(3)
P(1)–Rh–C(33)	90.3(1)		

[a] Numbers in parentheses are estimated standard deviations in the least significant digits.

(22) Structure done at the University of Toledo.
(23) Bennett, M. J.; Donaldson, P. B. *J. Am. Chem. Soc.* **1971**, *93*, 3307.
(24) Bennett, M. J.; Donaldson, P. B. *Inorg. Chem.* **1977**, *16*, 1581.
(25) Bennett, M. J.; Donaldson, P. B. *Inorg. Chem.* **1977**, *16*, 1585.
(26) Bennett, M. J.; Donaldson, P. B. *Inorg. Chem.* **1977**, *16*, 655.
(27) Bonnet, J. J.; Kalck, P.; Poilblanc, R. *Inorg. Chem.* **1977**, *16*, 1514.
(28) Kessler, J. M.; Nelson, J. H.; Frye, J. S.; DeCian, A.; Fischer, J. *Inorg. Chem.* **1993**, *32*, 1048.
(29) Osakada, K.; Hataya, K.; Yamamoto, T. *Inorg. Chem.* **1993**, *32*, 2360.

The reactions proceed smoothly, and generally only single substitution is observed. The reactant need posses only one activated fluorine for the substitution; in that case the substituent is non-fluorinated. The substituted iminophosphoranophosphines readily form stable complexes with transition metals exemplified by their complexes with Rh^{I}.

Experimental Section

All experimental manipulations were performed under an atmosphere of dry argon using Schlenk techniques. Solvents were dried and distilled prior to use. Toluene, acetonitrile, and dichloromethane were distilled from Na, CaH_2, and P_4O_{10} respectively. These solvents were purged with dry argon for at least 0.5 h before use. Commercial (Aldrich) supplies of dppm, Me_3SiN_3, 2,4-dinitrofluorobenzene, 1,5-difluoro-2,4-dinitrobenzene, 1,4-dicyanotetrafluorobenzene, 1,3-dicyanotetrafluorobenzene, and 1,2-dicyanotetrafluorobenzene were used as obtained. Compounds **1** and **2** and their corresponding Rh(I) complexes $R\overline{N{=}PPh_2CH_2PPh_2Rh(CO)Cl}$ (R = $SiMe_3$ (**11**), $C_6F_4(CN)$ (**10**)) were prepared as previously described.[11-14,16]

Synthesis of 2,4-$(NO_2)_2C_6H_3N{=}PPh_2CH_2PPh_2$ (3). To a solution of $Me_3SiN{=}PPh_2CH_2PPh_2$ (**1**) (3.72 g; 7.90 mmol) in dry toluene (100 mL) was added dropwise a solution of 1-F-2,4-$(NO_2)_2C_6H_3$ (1.47 g; 7.93 mmol) also in toluene (50 mL). The reaction mixture was refluxed for 12 h before the solvent was removed in vacuo to leave a yellow crystalline solid. This crude product was crystallized from acetonitrile to obtain the pure compound **3** (yield 4.0 g; 90%; yellow crystals; mp 198 °C). Anal. Calcd for $C_{31}H_{25}N_3O_4P_2$: C, 65.85; H, 4.43; N, 7.44. Found: C, 66.00; H, 4.40; N, 7.46. MS (EI, *m/z*): 565 (M^+, 100%). ^1H NMR ($CDCl_3$): phenyl rings, δ 7.20, 7.56, 7.80 (m, 20H); PCH_2P methylene, δ 3.35 (d, 2H, $^2J_{HP}$ = 12.50 Hz).

Synthesis of 5-F-2,4-$(NO_2)_2C_6H_2N{=}PPh_2CH_2PPh_2$ (4). To a solution of $Me_3SiN{=}PPh_2CH_2PPh_2$ (**1**) (3.26 g; 6.91 mmol) in dry toluene (100 mL) was added a solution of 1,5-$(F)_2$-2,4$(NO_2)_2C_6H_2$ (1.42 g; 6.95 mmol) also in toluene (50 mL). The reaction mixture was refluxed for 12 h before the solvent was removed in vacuo to leave an orange-red crystalline solid, which was recrystallized from acetonitrile to obtain the pure compound **4** (yield 3.78 g; 94%; orange-red cubic crystals; mp 200 °C). Anal. Calcd for $C_{31}H_{24}FN_3O_4P_2$: C, 63.80; H, 4.11; N, 7.20. Found: C, 63.82; H, 4.40; N, 7.23. MS (EI, *m/z*): 583 (M^+, 100%). ^1H NMR ($CDCl_3$): phenyl rings, δ 7.22, 7.71, 7.85 (m, 20H); PCH_2P methylene, δ 3.38 (d, 2H, $^2J_{HP}$ = 12.5 Hz). ^{19}F NMR ($CDCl_3$): δ −111.90 (m, 1F).

Synthesis of 2,5-$(CN)_2C_6F_3N{=}PPh_2CH_2PPh_2$ (5) and 3,4-$(CN)_2C_6F_3N{=}PPh_2CH_2PPh_2$ (6). The synthesis of **5** is typical: to a solution of $Me_3SiN{=}PPh_2CH_2PPh_2$ (**1**) (2.72 g; 5.77 mmol) in dry toluene (100 mL) was added dropwise a solution of 1,4-$(CN)_2C_6F_4$ (1.17 g; 5.82 mmol) in the same solvent. The reaction mixture was refluxed for 16 h before the solvent was removed in vacuo to obtain a pale yellow crystalline solid, which was recrystallized from acetonitrile to obtain the pure compound **5** (yield 3.14 g; 94%; pale yellow cubic crystals; mp 176 °C). Anal. Calcd for $C_{33}H_{22}F_3N_3P_2$: C, 68.39; H, 3.83; N, 7.25. Found: C, 68.42; H, 3.84; N, 7.26. MS (EI, *m/z*): 579 (M^+, 100%). ^1H NMR ($CDCl_3$): phenyl rings, δ 7.10, 7.42, 7.85 (m, 20H); PCH_2P methylene, δ 3.35 (dd, 2H, $^2J_{HP^v}$ = 12 Hz, $^2J_{HP^{III}}$ = 2.5 Hz). ^{19}F NMR ($CDCl_3$) (F ortho, meta, or para relative to the imino substituent): $\delta(F_o)$ −121.3 (a broad multiplet, 1F, $^4J_{P^vF_o}$ = 10 Hz), $\delta(F_p)$ −134.9 (four sets of doublets, 1F, $^4J_{F_oF_p}$ = 13, $^5J_{F_mF_p}$ = 21, $^6J_{P^vF_p}$ = 4 Hz)), $\delta(F_m)$ −148.0 (appears as a doublet of doublets, 1F, $^5J_{F_oF_m}$ = 8 Hz, no resolvable J_{PF}).

6 was synthesized in a similar fashion. ^1H NMR ($CDCl_3$): phenyl rings, δ 7.1, 7.4, 7.8 (m, 20H); PCH_2P methylene, δ 3.47 (d, 2H, $^2J_{HP^v}$ = 12.1 Hz, $^2J_{HP^{III}}$ = nr). ^{19}F NMR ($CDCl_3$): $\delta(F_o$ (adjacent to CN)) −117.7 (a doublet of triplets, 1F, $^4J_{F_oF_o}$ = 22.0, $^5J_{F_oF_m}$ = 7.0, $^4J_{P^vF_o}$ = 6 Hz), $\delta(F_{o'})$ −139.0 (doublet of triplets, 1F, $^3J_{F_mF_o}$ = 22.0, $^4J_{P^vF_o}$ = 6 Hz), $\delta(F_m)$ −133.5 (appears as a doublet of doublets, 1F; no J_{PF} resolved).

Synthesis of 2,4-$(NO_2)_2C_6H_3N{=}PPh_2CH_2PPh_2Rh(CO)Cl$ (7). A solution of **3** (0.35 g; 6.1 mmol) in dry dichloromethane (50 mL) was added dropwise at 25 °C to a solution of $[Rh(CO)_2Cl]_2$ (0.12 g; 3.07 mmol) in the same solvent (20 mL). The reaction mixture was stirred at this temperature for 4 h before the solvent was removed in vacuo to yield a brown solid, which was then crystallized from CH_2Cl_2–hexane (2:1) to obtain pure complex **7** as a dichloromethane solvate (yield 0.39 g; 88%; brown cubic crystals; mp 196 °C dec). Anal. Calcd for $C_{33}H_{27}Cl_3N_3O_5P_2Rh(7{\cdot}CH_2Cl_2)$: C, 48.56; H, 3.30; N, 5.15; Cl, 13.04. Found: C, 48.60; H, 3.32; N, 5.16; Cl, 13.10. ^1H NMR ($CDCl_3$): phenyl rings, δ 7.23, 7.46, 7.84 (m, 20H); PCH_2P methylene, 3.82 (dd, 2H, $^2J_{HP}$ = 12.10, 7.65 Hz).

The reactions of $F(NO_2)_2C_6H_2N{=}PPh_2CH_2PPh_2$, **4**, and $(CN)_2C_6F_3N{=}PPh_2CH_2PPh_2$, **5**, with $[Rh(CO)_2Cl]_2$ were carried out under experimental conditions similar to those described above to obtain the dichloromethane solvates of $F(NO_2)_2C_6H_2N{=}PPh_2CH_2PPh_2Rh(CO)Cl$, **8**, and $(CN)_2C_6F_3N{=}PPh_2CH_2PPH_2Rh(CO)Cl$, **9**, respectively.

8·CH_2Cl_2: Yield 85%; brown microcrystalline; mp 206 °C dec. Anal. Calcd for $C_{33}H_{26}Cl_3FN_3O_5P_2Rh$: C, 47.46; H, 3.11; N, 5.03; Cl, 12.74. Found: C, 47.50; H, 3.14; N, 5.05; Cl, 12.82. ^1H NMR ($CDCl_3$): phenyl rings, δ 7.25, 7.55, 7.82 (m, 20H); PCH_2P methylene, δ 3.80 (dd, 2H, $^2J_{HP}$ = 11.20, 7.10 Hz). ^{19}F NMR ($CDCl_3$): δ − 110.29 (m, 1F).

9·CH_2Cl_2: Yield 82%; yellow microcrystalline; mp 178 °C dec. Anal. Calcd for $C_{35}H_{24}Cl_3F_3N_3OP_2Rh$: C, 50.58; H, 2.89; N, 5.05; Cl, 12.80. Found: C, 50.55; H, 2.83; N, 5.04; Cl, 12.92. ^1H NMR ($CDCl_3$): phenyl rings, δ 7.30, 7.47, 7.86 (m, 20H); PCH_2P methylene, 3.45 (t, 11.25 Hz). ^{19}F NMR ($CDCl_3$): δ −152.17 (m 1F), −138.47 (m, 1F), −124.40 (m, 1F).

Crystallography

Crystal structures of the phosphine–phosphinimine compounds **2**, **4**, and **10** were carried out on two different Enraf-Nonius CAD4 automated diffractometers, each equipped with a Mo X-ray tube and graphite monochromator. The relevant collection data are given in Table II.

Data Collection for 2.[18] A crystal of **2** was mounted on a glass fiber with epoxy. Automated peak search and reflection indexing programs[30] in conjunction with a cell reduction program showed the crystals of **2** to be monoclinic; the systematic absences (*h0l*, *l* odd; *0k0*, *k* odd) uniquely identified the space group as $P2_1/c$ (No. 14). The cell constants and orientation matrix were obtained from a least-squares refinement of the setting angles of 25 reflections in the range $9.7 < \theta < 19.9°$.

Intensity data were collected at room temperature (23 °C) using an ω–2θ scan of fixed speed (4.0° min^{-1} (in θ)). The scan varied as a function of θ to compensate for α_1–α_2 wavelength dispersion [ω scan width = (0.75 + 0.35 tan θ)°]. Peak backgrounds were measured from scans by extending scans by 25% on either side giving a peak-to-background counting time ratio of 2:1. Intensity measurements were made to a maximum 2θ of 50°. Monitoring three standard reflections at 120-min intervals showed a minor decline of intensity. No decay correction was applied.

Data Reduction for 2. A total of 9134 reflections were collected, and Lorentz and polarization factors were applied using the relations

$$I = r(S - 2B)Lp$$

$$\sigma(I) = [r(S + 4B) + (0.04I)^2]^{1/2}/Lp$$

where r = scan rate, S is total scan count, B is total background count, and Lp is the combined Lorentz and polarization factor.

Structure Solution and Refinement of 2. The structure of **2** was solved using the direct methods program MITHRIL.[31] The positions of most of the non-hydrogen atoms were evident from the generated *E*-map. The remaining atoms were located from a set of difference Fourier maps. Adjustment[32] of atomic parameters was carried out by full-matrix least-squares refinement on F minimizing the function $\sum w(|F_o| - |F_c|)^2$. The weight w is given by $w = 4F_o^2/\sigma^2(F_o^2)$. The neutral-atom scattering factors were calculated from the analytical expression for the scattering factor curves.[33] The f' and f'' components of anomalous dispersion[34] were included in the calculations of all non-hydrogen atoms.

(30) The diffractometer programs are those supplied by Enraf-Nonius for operating the CAD4F diffractometer at the University of Alberta. Some local modifications at the University of Alberta were made by Dr. R. G. Ball.

(31) Gilmore, C. J. MITHRIL 83. A Multiple Solution Direct Methods Program. University of Glasgow, 1983.

(32) The computer programs used in the determination at the University of Alberta include the Enraf-Nonius Structure Determination Package, Version 3 (1985, Delft, The Netherlands) adapted for a SUN Microsystems 3/160 computer, and several locally written (Alberta) programs by Dr. R. G. Ball.

(33) Cromer, D. T.; Waber, J. T. *International Tables for X-ray Crystallography*; Kynoch Press: Birmingham, U.K., 1974; Vol. IV, Table 2.2B (present distributor D. Reidel, Dordrecht, The Netherlands).

(34) Cromer, D. T.; Waber, J. T. *International Tables for X-ray Crystallography*; Kynoch Press: Birmingham, U.K., 1974; Vol. IV, Table 2.3.1 (present distributor D. Reidel, Dordrecht, The Netherlands).

All hydrogen atoms were generated at idealized calculated positions by assuming a C–H bond length of 0.95 Å and the appropriate sp^2 or sp^3 geometries. These atoms were then included in the calculations with fixed, isotropic Gaussian parameters 1.2 times those of the attached atoms and were constrained to "ride" on the attached atoms.

The refinement of the coordinates and isotropic U's for all non-hydrogen atoms was continued to convergence. At that stage, the data were corrected for absorption (and other systematic errors) using a scheme based on the absorption surface (Fourier filtering) method of Walker and Stuart.[35] The maximum and minimum correction factors applied to F_o were 1.2654 and 0.2909. After averaging over $2/m$ symmetry (R-merge of F for all data is 0.108), a total of 5032 averaged reflections remained, of which 3190 had $I > 1.50\sigma(I)$. The refinement was continued with use of anisotropic Gaussian displacement parameters for the non-hydrogen atoms. In the final cycle 361 parameters were refined using 3190 observations with $I > 1.50\sigma(I)$, and the largest shift/error was less than 0.01. The final goodness-of-fit was 2.13, and $R_1 = 0.070$ and $R_2 = 0.080$. The density of the highest peak in the final difference Fourier map was 0.25(6) e/Å^3.

Data Collection for 4.[18] The crystal was mounted on a glass fiber and coated with epoxy. Data were collected in a manner similar to that for **2** except at −80 °C. The systematic absences (hkl, $h + k$ odd; $h0l$, l odd) suggested a monoclinic cell, and the magnitude of the unit cell suggested space groups Cc (No. 9) or $C2/c$ (No. 15) with one molecule in the asymmetric unit. The selection of Cc was confirmed by successful refinement in this group. Cell constants were obtained from 25 reflections in the range $11.0 < \theta < 20.2°$. Scans (ω–2θ) were done at 2.0° min^{-1} (in θ); ω scan width = $(1.00 + 0.347 \tan\theta)°$. No significant decline was observed in intensity of standard scans during data collection. A total of 9306 reflectons were collected. Lorentz and polarization factors were calculated as given above.

Structure Solution and Refinement of 4. The positions of the P atoms were derived from a three-dimensional Patterson map, and R began at 0.37. The remaining non-hydrogen atoms were located from a set of difference Fourier maps. Least-squares refinement and generation of hydrogen atom positions proceeded in the manner described for **2** as did the correction for absorption and other systematic errors (the maximum and minimum correction factors applied to F_o were 1.1138 and 0.8443). After averaging over $2/m$ symmetry (R-merge on F is 0.124) and deletion of the systematic absences, there were 4472 averaged reflections, 2099 with $I > 1.50\sigma(I)$. The refinement was continued with use of anisotropic Gaussian displacement parameters for the non-hydrogen atoms. In the final cycle, 368 parameters were refined using the 2099 observations with $I > 1.50\sigma(I)$, and the largest shift/error ratio was less than 0.01. The final goodness-of-fit was 1.14, and $R_1 = 0.052$ and $R_2 = 0.049$. The highest peak in the final difference Fourier map has a density of 0.16(4) e Å^{-3}.

Data Collection for 10.[22] The crystal[12] was mounted on a glass fiber. Cell constants were obtained from least-squares refinement, using the setting angles of 25 reflections in the range $11 < \theta < 12°$. From the systematic absences (hkl, $h + k$ = odd; $h0l$, l = odd) and from subsequent least-squares refinement, the space group was determined to be $C2/c$ (No. 15).

The (ω–2θ) scan rate was variable ranging from 1 to 7°/min (in ω). Data were collected to a maximum 2θ of 52.0°, with the ω scan width = $0.6 + 0.34 \tan\theta$. Moving-crystal moving-counter background counts were made by scanning an additional 25% above and below this range, and the backgrounds were obtained by analysis of the scan profile.[36] The horizontal counter aperture width ranged from 1.8 to 1.9 mm; the vertical aperture was set at 3.0 mm. The small apertures and narrow slit width were chosen to optimize resolution. For intense reflections an attenuator was automatically inserted in front of the detector; the attenuator factor was 13.5.

Data Reduction for 10. A total of 7648 reflections were collected, of which 7537 were unique. An anisotropic decay correction was applied, the correction factors on I ranging from 0.973 to 1.040.

An empirical absorption correction based on a series of ψ-scans was applied to the data; relative transmission coefficients ranged from 0.888 to 0.999. Lorentz and polarization corrections were applied to the data. Intensities of equivalent reflections were averaged. The agreement factors for the averaging of the 183 observed and accepted reflections were 1.1% based on intensity and 1.0% based on F_o.

Structure Solution and Refinement for 10. The structure was solved using the Patterson heavy-atom method, which revealed the position of the Rh atom. The remaining atoms were located in succeeding difference Fourier syntheses. Hydrogen atoms were included in the refinement but restrained to ride on the atom to which they are bonded. The structure was refined in full-matrix least-squares minimizing $\sum w(|F_o| - |F_c|)^2$, where $w = 4F_o^2/\sigma^2(F_o^2)$. All calculations were done using MolEN.[37,38]

Scattering factors were taken from Cromer and Waber.[33] Anomalous dispersion effects were included in F_c;[39] the values for $\Delta f'$ and $\Delta f''$ were those of Cromer.[34] Only the 5948 reflections having intensities greater than 3.0 times their standard deviation were used in the refinements. The final cycle of refinement included 433 variable parameters and converged (largest parameter shift was 0.25 times esd) with unweighted and weighted agreement factors of $R_1 = 0.036$ and $R_2 = 0.056$. The standard deviation of an observation of unit weight was 1.94. The highest peak in the final difference Fourier had a height of 0.99(7) e/Å^3.

Acknowledgment. We thank the Natural Sciences and Engineering Research Council of Canada for support at the University of Alberta and (for A.A.P.) the College of Arts and Sciences at the University of Toledo. We also thank Vivian Mozol and Jin Li of the University of Alberta for checking NMR data of **5** and **6**.

Supplementary Material Available: For **2**, tables of crystallographic data (Table S1), selected bond lengths (S2), selected interatomic angles (S3), torsional angles (S4), positional and anisotropic and equivalent isotropic Gaussian displacement parameters (S5), root-mean-square amplitudes of anisotropic Gaussian displacement parameters (S6), weighted least-squares planes (S7), and derived Gaussian positional parameters for hydrogen atoms (S8), for **4**; tables of crystallographic data (S9), selected bond lengths (S10), selected interatomic angles (S11), torsional angles (S12), atomic coordinates and anisotropic and equivalent isotropic Gaussian displacement parameters (S13), root-mean-square amplitudes of anisotropic Gaussian displacement parameters (S14), derived positional parameters for hydrogen atoms (S15), and weighted least-squares planes (S16), and, for **10**, tables of crystallographic data (S17), calculated hydrogen atom positional parameters (S18), general displacement parameter expressions (S19), bond distances (S20), bond angles (S21), and least-squares planes (S22) (26 pages). Ordering information is given on any current masthead page.

(35) Walker, N.; Stuart, D. *Acta Crystallogr.* **1983**, *A39*, 158.
(36) Blessing, H.; Coppens, P.; Becker, P. *J. Appl. Crystallogr.* **1974**, *7*, 488.
(37) Fair, K. MolEN, An Interactive Intelligent System for Crystal Structure Analysis, User's Manual. Enraf-Nonius, Delft, Holland, 1989.
(38) All calculations were performed on a VAXStation 3100.
(39) Ibers, J. A.; Hamilton, W. C. *Acta Crystallogr.* **1964**, *17*, 781.